CHEMISTRY
A EUROPEAN JOURNAL

DOI: 10.1002/chem.201000174

Carbodicarbenes and Related Divalent Carbon(0) Compounds

Susanne Klein, Ralf Tonner, and Gernot Frenking*[a]

Dedicated to Professor Wolfgang Petz on the occasion of his 70th birthday

Abstract: Quantum-chemical calculations using DFT and ab initio methods have been carried out for fourteen divalent carbon(0) compounds (carbones), in which the bonding situation at the two-coordinate carbon atom can be described in terms of donor–acceptor interactions L→C←L. The charge- and energy-decomposition analysis of the electronic structure of compounds **1**–**10** reveals divalent carbon(0) character in different degrees for all molecules. Carbone-type bonding L→C←L is particularly strong for the carbodicarbenes **1** and **2**, for the "bent allenes" **3a**, **3b**, **4a**, and **4b**, and for the carbocarbenephosphoranes **7a**, **7b**, and **7c**. The last-named molecules have very large first and large second proton affinities. They also bind two BH_3 ligands with very high bond energies, which are large enough that the bis-adducts should be isolable in a condensed phase. The second proton affinities of the complexes **5**, **6**, and **8**–**10** bearing CO or N_2 as ligand are significantly lower than those of the other molecules. However, they give stable complexes with two BH_3 ligands and thus are twofold Lewis bases. The calculated data thus identify **1**–**10** as carbones L→C←L in which the carbon atom has two electron pairs. The chemistry of carbones is different from that of carbenes because divalent carbon(0) compounds CL_2 are π donors and thus may serve as double Lewis bases, while divalent carbon(II) compounds are π acceptors. The theoretical results point toward new directions for experimental research in the field of low-coordinate carbon compounds.

Keywords: bonding analysis · carbon · carbones · density functional calculations · donor–acceptor systems

Introduction

The recent revival of carbodiphosphorane chemistry[1–3] and the interpretation of $C(PR_3)_2$ as divalent carbon(0) compounds CL_2[3] in which a carbon atom retaining all four valence electrons as two lone pairs is bonded to two σ-donor ligands (Scheme 1) sparked intensive theoretical[4–11] and experimental[10–14] investigations of this hitherto unrecognized class of compounds, which has been the subject of two recent reviews.[15,16] A highlight of this work was the advent of carbodicarbenes $C(NHC)_2$ as a new type of divalent carbon(0) compounds CL_2 with N-heterocyclic carbenes (NHCs) as ligands, which were theoretically predicted to be stable molecules.[4–6] Bertrand and co-workers subsequently synthesized[12] the first stable carbodicarbene, while further studies by Fürstner et al.[10,13] proved the validity of the carbon(0) concept for this promising class of compounds. The high electron density and availability of two lone pairs of electrons at the central carbon atom suggest new and unusual ligand properties which are waiting to be explored.[14–16]

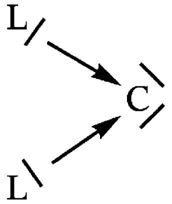

Scheme 1. Schematic representation of the bonding situation in divalent carbon(0) compounds.

The theoretical studies[4–11] on the electronic structure of compounds CL_2 suggested a wide scale of bonding situations between divalent carbon(0) compounds such as carbodiphosphoranes $C(PR_3)_2$ and carbodicarbenes $C(NHC)_2$ having two lone-pair orbitals at the central carbon atom and divalent carbon(II) compounds with only one electron lone pair at the carbon atom. The latter species are carbenes, while the term carbone has been proposed for divalent

---

[a] Dipl.-Chem. S. Klein, Dr. R. Tonner, Prof. G. Frenking
Fachbereich Chemie, Philipps-Universität Marburg
Hans-Meerwein-Strasse, 35043 Marburg (Germany)
E-mail: frenking@chemie.uni-marburg.de

Supporting information for this article is available on the WWW under http://dx.doi.org/10.1002/chem.201000174. It contains Cartesian coordinates and total energies of all compounds, figures of the optimized structures of the free ligands L and the adducts with one and two BH_3 molecules, tables with BP86/TZVPP and SCS-MP2/TZVPP values for PA and D_e of BH_3 complexes as well as NBO results for the BH_3 complexes.

carbon(0) compounds.[7,16] Divalent carbon(0) behavior may even be found as "hidden"[4–6] feature in formally tetravalent carbon(IV) compounds such as tetraaminoallenes $(NR_2)_2C{=}C{=}C(NR_2)_2$,[4–6] in which the central carbon atom is a strong donor which binds CO_2[17] in an adduct that resembles the complex $(PPh_3)_2C\text{-}CO_2$, which was recently isolated and characterized by X-ray structure analysis.[1]

The new findings suggest that other organic compounds may exist which have either not been synthesized yet or which have not been recognized as carbones CL_2. Here we report on a computational study on a set of molecules **1**–**10** (Scheme 2) to determine whether they exhibit chemical reactivity that is typical for divalent carbon(0) compounds. To this end we calculated the first and second proton affinities of the molecules, which were suggested as probes for divalent carbon(0) character.[4,6,7,16] We also estimated the first and second donor strengths of **1**–**10** with respect to a strong Lewis base by calculating the geometries and bond-dissociation energies of the complexes with one and two BH_3 ligands. Finally, we present a thorough analysis of the electronic structure of the calculated molecules using charge- and energy-decomposition methods.

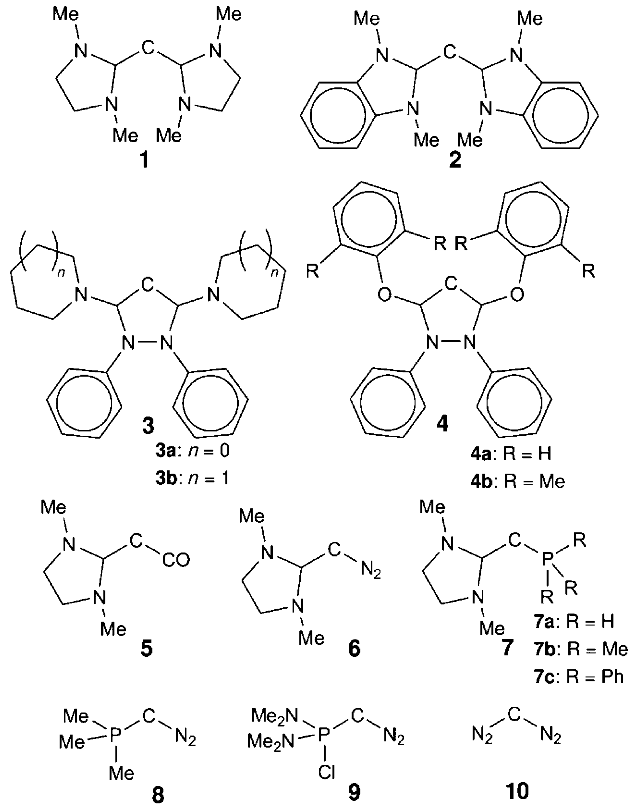

Scheme 2. Compounds investigated in this work: carbodicarbenes **1**, **2**; "bent allenes" **3**, **4**; carbones CLL′ with the ligands L, L′ = NHC, PR_3, CO, and N_2 (**5**–**10**).

The choice of the systems was guided by two aspects: 1) investigation of recently synthesized compounds such as benzannelated carbodicarbene **2**[12] and "bent allenes"[11,12,14] **3** and **4b** and 2) inclusion of complexes with mixed ligands CLL′ **5**–**9**. Carbodicarbene **1**, which has saturated NHC ligands, was included in this work because prior studies focused on $C(NHC)_2$ with unsaturated ligands.[4–6] Compound **2** was the first experimentally observed and characterized[12] carbodicarbene, but it has not been the subject of a theoretical study. While the carbon(0) character of **2** and model compound **1** is undisputed, the interpretation of the bonding situation in "bent allenes" **3** and **4b**, which were recently synthesized by Bertrand and co-workers,[11,12] has been controversially debated.[18,19] A recent experimental and theoretical study established strong exocyclic delocalization in these molecules, which have distinct carbon(0) character.[11] Compounds **5**–**9** with mixed ligands L and L′ are new variants of the systems CL_2, where L is NHC, CO, or PR_3, which were previously investigated by us.[3–7,16] Molecules **6**, **8**, and **9** feature N_2 as a ligand in CL_2. They were included in our study because we found in the literature that compounds with the general formula $C(PR_3)(N_2)$ were already synthesized by Bertrand and co-workers more than 20 years ago.[20] These were described as phosphacumulenes with double bonds at carbon $R_3P{=}C{=}N_2$, which was at that time the common description for such molecules.[21] We note that the first stable carbene, which was synthesized by Bertrand and co-workers in 1988, was originally depicted to be a λ^5-phosphaacetylene $R_2P{\equiv}C\text{-}SiMe_3$ on the basis of NMR spectroscopy.[22] It was only later recognized that the molecule is better described as a carbene $R_2P{-}C{-}SiMe_3$.[23] The homoleptic parent system for the dinitrogen compounds is $C(N_2)_2$ (**10**), which was theoretically predicted as stable species by Pyykkö and Runeberg in 1991.[24]

Methods

Geometry optimizations without symmetry constraints were carried out with the Gaussian 03[25] optimizer[26] in conjunction with Turbomole 5[27] energies and gradients at the BP86[28]/def-SVP[29] level of theory. Stationary points were characterized by calculating the Hessian matrix analytically at this level of theory. Thermodynamic corrections and Kohn–Sham orbitals were taken from these calculations. The standard state for all thermodynamic data is 298.15 K and 1 atm. Single-point energies at the BP86/def-SVP (in the following called SVP) optimized geometries were calculated with the MP2 method[30] with application of the frozen-core approximation for non-valence-shell electrons and with BP86 and the def2-TZVPP[31] basis set (in the following called TZVPP). Coupled-cluster[32a–g] energies at the CCSD(T)/TZVPP level were calculated for some molecules with the program package Molpro2006.[32h] For the BP86 and the MP2 calculations the resolution of the identity method[33] was applied. MP2 energies were also calculated with inclusion of the spin-component-scaled (SCS) correction proposed by Grimme[34] by applying the standard parameters. The NBO[35–37] analyses were carried out with the internal module of Gaussian 03 at the BP86/TZVPP//BP86/def-SVP level of theory without using the resolution of the identity approximation.

For bonding analyses in terms of energy-decomposition analysis, the geometries of molecules **1**–**10** were also optimized with the program package ADF2006.01.[38] As above, BP86 was chosen with uncontracted Slater-type orbitals (STOs) as basis functions. The basis sets for all elements have triple-ζ quality augmented by two sets of polarization functions (ADF basis set TZ2P[39]). Core electrons (i.e., 1s for second- and [He]2s2p for third-row atoms) were treated by the frozen-core approximation. This level of theory is denoted BP86/TZ2P. An auxiliary set of s, p, d, f, and g STOs was used to fit the molecular densities and to represent the Coulomb and exchange potentials accurately in each SCF cycle.[40] Scalar relativistic effects were incorporated by applying the zeroth-order regular approximation (ZORA)[41,42] in all calculations undertaken with ADF. The interatomic interactions were investigated by means of an energy-decomposition analysis (EDA) developed independently by Morokuma[43] and by Ziegler and Rauk.[44] The bonding analysis focuses on the instantaneous interaction energy ΔE_{int} between two fragments A and B in the particular electronic reference state and in the frozen geometry of the molecule AB. The interaction energy can be divided into three main components [Eq. (1)],

$$\Delta E_{\mathrm{int}} = \Delta E_{\mathrm{elstat}} + \Delta E_{\mathrm{Pauli}} + \Delta E_{\mathrm{orb}} \tag{1}$$

where $\Delta E_{\mathrm{elstat}}$ is the electrostatic interaction energy between the fragments, which are calculated by means of the frozen electron density distribution of the fragments in the geometry of the molecules. $\Delta E_{\mathrm{Pauli}}$ refers to the repulsive interactions between the fragments, which are caused by the fact that two electrons with the same spin cannot occupy the same region in space. $\Delta E_{\mathrm{Pauli}}$ is calculated by enforcing the Kohn–Sham determinant on the superimposed fragments to obey the Pauli principle by antisymmetrization and renormalization. The stabilizing orbital interaction term ΔE_{orb} is calculated in the final step of the energy partitioning analysis when the Kohn–Sham orbitals relax to their optimal form. This term can be further partitioned into contributions of orbitals belonging to different irreducible representations of the point group of the interacting fragments. The interaction energy ΔE_{int} can be used to calculate the bond-dissociation energy $-D_e$ by adding ΔE_{prep}, which is the energy necessary to promote the fragments from their equilibrium geometry to the geometry in the compounds [Eq. (2)].

$$-D_e = \Delta E_{\mathrm{prep}} + \Delta E_{int} \tag{2}$$

Further details on the EDA method[45,46] and its application to the analysis of the chemical bond[47,48] can be found in the literature.

Results and Discussion

Geometries and energies: The optimized geometries of compounds **1**–**10** are shown in Figure 1 together with the calculated values for the most important bond lengths and angles. Experimental data from X-ray analyses are given for **2**,[12] **3a**,[14] and **4b**.[14] For **3a** only a crystal structure of the $LiBF_4$ adduct is published.[14] The agreement between the calculated structures and the experimental data is very good. The difference between the theoretical (142.5°) and experimental (134.8°) values for the C2a-C1-C2b angle in **2** is probably due to intermolecular interactions in the solid state. It has previously been shown that the bending potential of carbon(0) compounds is very shallow.[4,5,16]

The calculated C1−C2 bonds of "bent allenes" **3** and **4** are about 0.04 Å longer than those of the carbodicarbenes **1** and

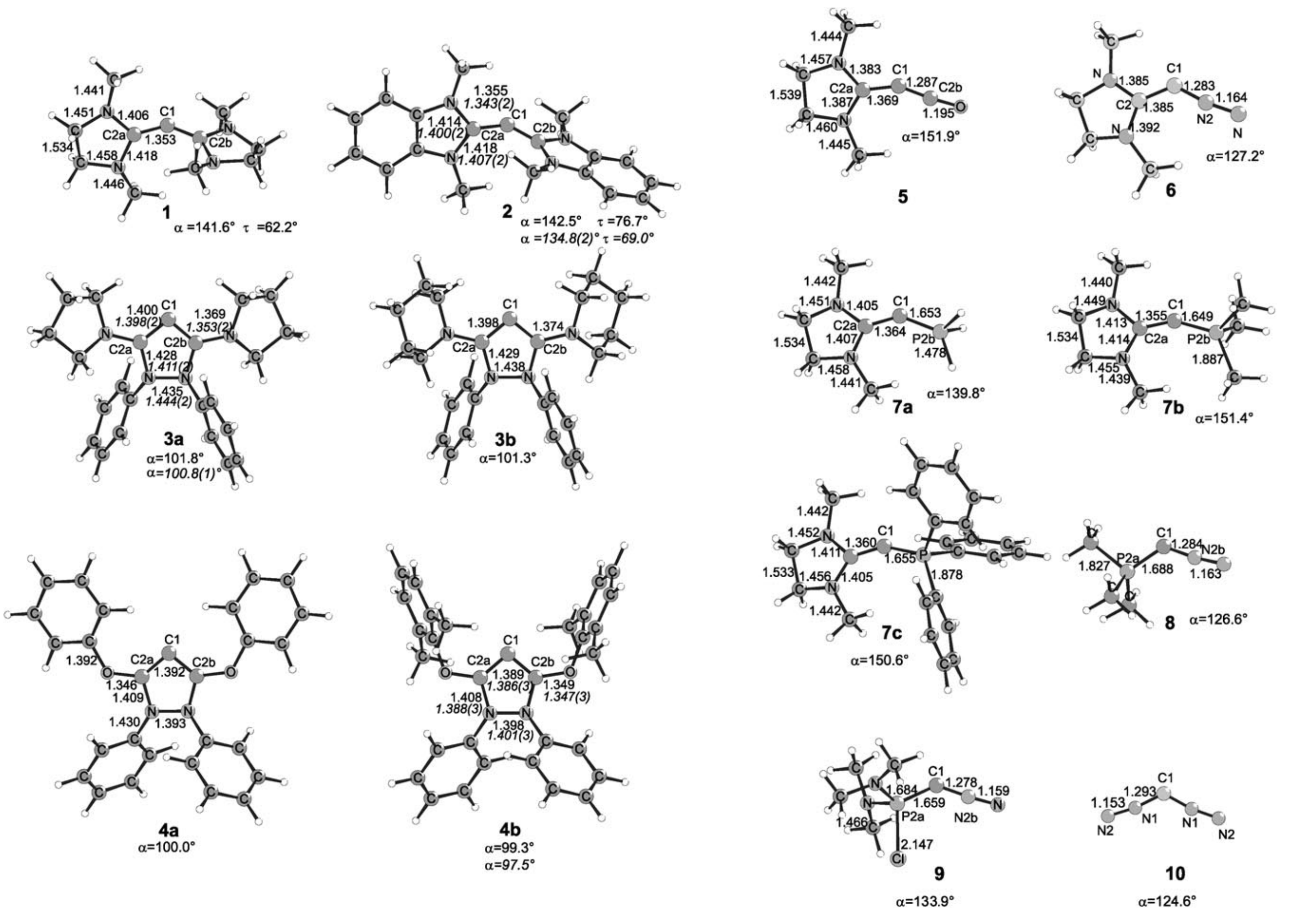

Figure 1. Optimized structures (bond lengths [Å] and angles [°]) of **1**–**10** at the BP86/SVP level of theory. Experimental data from X-ray analyses for **2**,[12] **3a**,[14] and **4b**[14] are given in parentheses. The experimental data of **3a** refer to the $LiBF_4$ adduct of the compound.

2, which is in agreement with the experimental values of **2** and **4b**. The mixed CLL′ systems **5**–**10** are all significantly bent, with bending angles between 124.6° for **10** and 151.9° for **5**. Note that the NHC−CL bonds in mixed complexes **5**–**7c** are always slightly longer than in the homoleptic adduct C(NHC)$_2$ (**1**) while the N$_2$−CL bonds in **6**, **8**, and **9** are always shorter than in C(N$_2$)$_2$ (**10**). The strongly bent equilibrium structures are a first hint that the investigated molecules may not be considered as classical (hetero-)cumulenes but might be further examples of divalent carbon(0) compounds. The N−N and C−O distances of the N$_2$ and CO ligands in **5**, **6**, and **8**–**10** are slightly longer than in free N$_2$ (1.112 Å) and CO (1.142 Å). This indicates some C→L (L = N$_2$, CO) π backdonation in these compounds.

Comparison of the calculated bending angles of carbones CL$_2$ and the π-acceptor strength of L suggest that there is a clear correlation between these two variables. The strong π acceptor CO leads to a quasilinear structure in carbon suboxide C(CO)$_2$, which has a bending angle in the gas phase of about 156°.[50b] The carbone C(N$_2$)$_2$ (**10**), which has the weaker π acceptor N$_2$ as ligand, has a much more acute angle of 124.6°, which is similar to the calculated (BP86/SVP) bending angles of 123.6° for C(PH$_3$)$_2$ and 126.6° for C(NHC$_H$)$_2$, where NHC$_H$ is an unsaturated NHC which has hydrogen atoms at the nitrogen atoms.[5] The larger bending angles calculated for C(PPh$_3$)$_2$ (135.0°) and C(NHC$_{Me}$)$_2$ (132.3°) may partly be caused by steric repulsion between the bulky ligands.[5] Steric repulsion between the ligands should be negligible in **5**, **6**, **8**, and **9**. The trend of the calculated bending angle in the latter compounds is in agreement with the π-acceptor model. The much more acute bending angles for **6** (127.2°) and **8** (126.6°) than for **5** (151.9°) can be explained by the effect of the strong π acceptor CO in the last-named species, which is replaced by N$_2$ in the other two. Compound **9** has a phosphane ligand bearing electronegative Cl and NMe$_2$ groups instead of the methyl groups of the PMe$_3$ ligand in **8**. This makes the phosphane ligand in **9** a better π acceptor than in **8**, and thus **9** has a more obtuse bending angle of 133.9° than **8** (126.6°).

Table 1 lists the calculated values for the bond-dissociation energy (BDE) of **1**–**10** for dissociation into a bare carbon atom in its ^{3}P electronic ground state and two ligands L and L′, predicted by DFT (BP86/TZVPP) and ab initio methods (MP2/TZVPP and SCS-MP2/TZVPP). In all cases BP86/SVP geometries were used. Theoretical BDEs which were previously reported for carbones and for the parent NHC are also given.[5] In general. agreement between the BP86/TZVPP values and the fairly accurate[34b] SCS-MP2/TZVPP results is good, except for molecules which carry CO or N$_2$ as ligands, the calculated bond energies (SCS-MP2/TZVPP) of which are significantly lower than the BP86/TZVPP values. The largest difference is found for C(N$_2$)$_2$ (**10**), for which SCS-MP2/TZVPP gives a BDE of only $D_e = 31.6$ kcal mol^{-1}, while the BP86/TZVPP value of $D_e = 72.6$ kcal mol^{-1} is much higher. The overall trends of the bond energies at the BP86/TZVPP and SCS-MP2/TZVPP levels are very similar, however.

To estimate the accuracy of the calculated BDEs we carried out additional energy calculations at the highly accurate CCSD(T)/TZVPP level for those molecules which are not too large for this expensive method using BP86/SVP optimized geometries. Table 1 shows that the SCS-MP2/TZVPP

Table 1. Dissociation energies D_e and energies including thermal and zero-point vibrational contributions D_0^{298} for the reaction C(LL′)→C (^{3}P)+L+L′ [kcal mol^{-1}]. All energy calculations were carried out with the TZVPP basis set on BP86/SVP geometries. The thermal and entropic contributions were taken from the BP86/SVP calculations.

			BP86		MP2		SCS-MP2		CCSD(T)	
L	L′	No.	D_e	D_0^{298}	D_e	D_0^{298}	D_e	D_0^{298}	D_e	D_0^{298}
NHC^s_{Me}	NHC^s_{Me}[b]	**1**	193.1	188.4	204.9	200.2	192.6	187.9	–	–
$NHCC^b_{Me}$	NHC^b_{Me}[c]	**2**	191.4	187.4	194.8	190.8	183.0	179.0	–	–
RCN(Ph)N(Ph)CR[d]		**3a**	197.6	194.1	206.9	203.4	196.5	193.0	–	–
RCN(Ph)N(Ph)CR[d]		**3b**	199.4	195.7	209.1	205.4	198.8	195.1	–	–
RCN(Ph)N(Ph)CR[d]		**4a**	198.3	194.8	204.4	200.8	191.8	188.2	–	–
RCN(Ph)N(Ph)CR[d]		**4b**	201.6	198.0	209.7	206.1	196.9	193.3	–	–
NHC^s_{Me}	CO	**5**	192.0	186.9	184.5	179.4	168.0	162.9	166.4	161.3
NHC^s_{Me}	N_2	**6**	141.8	137.0	134.9	130.1	121.0	116.2	112.7	107.9
NHC^s_{Me}	PH_3	**7a**	148.0	143.6	151.9	147.5	141.7	137.2	135.3	130.9
NHC^s_{Me}	PMe_3	**7b**	159.8	155.8	168.7	164.7	157.0	153.0	–	–
NHC^s_{Me}	PPh_3	**7c**	158.0	154.0	171.6	167.6	158.6	154.7	–	–
PMe_3	N_2	**8**	112.9	108.8	104.0	99.9	91.4	87.4	84.5	80.4
$PCl(NMe_2)_2$	N_2	**9**	111.9	108.2	106.5	102.8	93.2	89.4	–	–
N_2	N_2	**10**	72.6	68.8	45.2	41.4	31.6	27.8	25.8	22.0
PH_3	PH_3	[a]	107.8	103.4	108.7	104.2	100.6	96.1	93.3	88.8
PMe_3	PMe_3	–[a]	135.8	132.3	145.3	141.8	134.6	131.1	129.0	125.5
PPh_3	PPh_3	–[a]	129.9	126.4	151.3	147.8	137.7	134.2	–	–
PPh_3	CO	–[a]	161.7	157.4	156.6	152.3	145.4	141.1	–	–
CO	CO	–[a]	175.7	170.8	154.8	149.8	142.3	137.3	136.0	131.1
NHC^u_{Me}	NHC^u_{Me}[e]	–[a]	178.9	175.2	181.5	177.7	170.3	166.5	–	–
HN=CH-CH=NH[f]		–[a]	171.8	168.1	170.4	166.7	161.5	157.8	158.6	154.9

[a] Values taken from reference [5]. [b] *N*-Methyl-substituted saturated NHC. [c] *N*-Methyl-substituted benzannelated NHC. [d] Bidentate fragment of cyclic species (see Figure S1, Supporting Information). [e] *N*-Methyl-substituted unsaturated NHC. [f] Bidentate fragment of cyclic NHC.

results show the best agreement with the CCSD(T)/TZVPP values. The theoretically predicted BDEs at the CCSD(T)/TZVPP level are 2–9 kcal mol^{-1} smaller than the SCS-MP2/TZVPP results. Since BP86/TZVPP and MP2/TZVPP give even larger bond energies than SCS-MP2/TZVPP, it follows that the BDEs at the first two levels are uniformly too high. The difference is particularly striking for $C(N_2)_2$ (**10**), for which the calculated enthalpy at the BP86/TZVPP level suggests rather strong donor–acceptor bonds, while the CCSD(T)/TZVPP results show that it is much less stable. However, the trends of the BDEs at the CCSD(T)/TZVPP level are the same as given by BP86/TZVPP.

The calculations suggest that the C→C donor–acceptor bonds of the saturated NHC^{s}_{Me} ligands in **1** and the benzannelated NHC^{b}_{Me} ligands in **2** are stronger than the bonds of the unsaturated NHC^{u}_{Me} ligand in $C(NHC^{u}_{Me})_2$ (Table 1). Even slightly stronger bonds are predicted for the cyclic “bent allenes” **3a**, **3b**, **4a**, and **4b**, which have the highest BDEs for dissociation of a bare carbon atom of all compounds listed in Table 1. The ligand fragments in the dissociation reactions of **3a**–**4b** are bis-carbenes in the singlet state with a *trans* configuration of the carbene substituents at the N−N bond (see Figure S1 in Supporting Information). Substitution of one saturated NHC^{s}_{Me} ligand in **1** gives the mixed carbones $(NHC^{s}_{Me})CL$, where L = CO (**5**), N_2 (**6**), PH_3 (**7a**), PMe_3 (**7b**), and PPh_3 (**7c**). Table 1 shows that the calculated BDEs exhibit the trend **5** > **7b** ≈ **7c** > **7a** > **6**. They all should be stable enough to be isolated in a condensed phase, because $(Me_3P)C(N_2)$ (**8**) and $[(Me_2N)_2ClP]C(N_2)$ (**9**) have much lower BDEs than **5**–**7**. Homologues of **8** and **9** which bear bulky substituents at the phosphane groups have been synthesized by Bertrand and co-workers.[20] It may be difficult, however, to isolate the homoleptic complex $C(N_2)_2$ (**10**) because of its rather weak donor–acceptor bonds.

Bonding analysis: The bonding situation in compounds **1**–**10** was investigated with NBO and frontier orbital analyses. The two highest-lying molecular orbitals of the investigated molecules are depicted in Figure 2. Visual inspection of the HOMO and HOMO−1 shows that the largest coefficient is always at the central carbon atom, which suggests that **1**–**10** could be classified as carbones. Quantitative data on the nature of the orbitals comes from the NBO analysis (Table 2).

Although the equilibrium structures of some molecules do not have a mirror plane, the shape of the frontier orbitals clearly reveals in all cases typical σ- and π-type character, because there is a local mirror plane in the vicinity of the central carbon atom. It is thus possible to classify the HOMO and HOMO−1 as σ and π orbitals even though there is no overall mirror plane in the molecule. Figure 2 shows that the HOMO of **1**, **2**, **6**, and **8**–**10** has (local) π

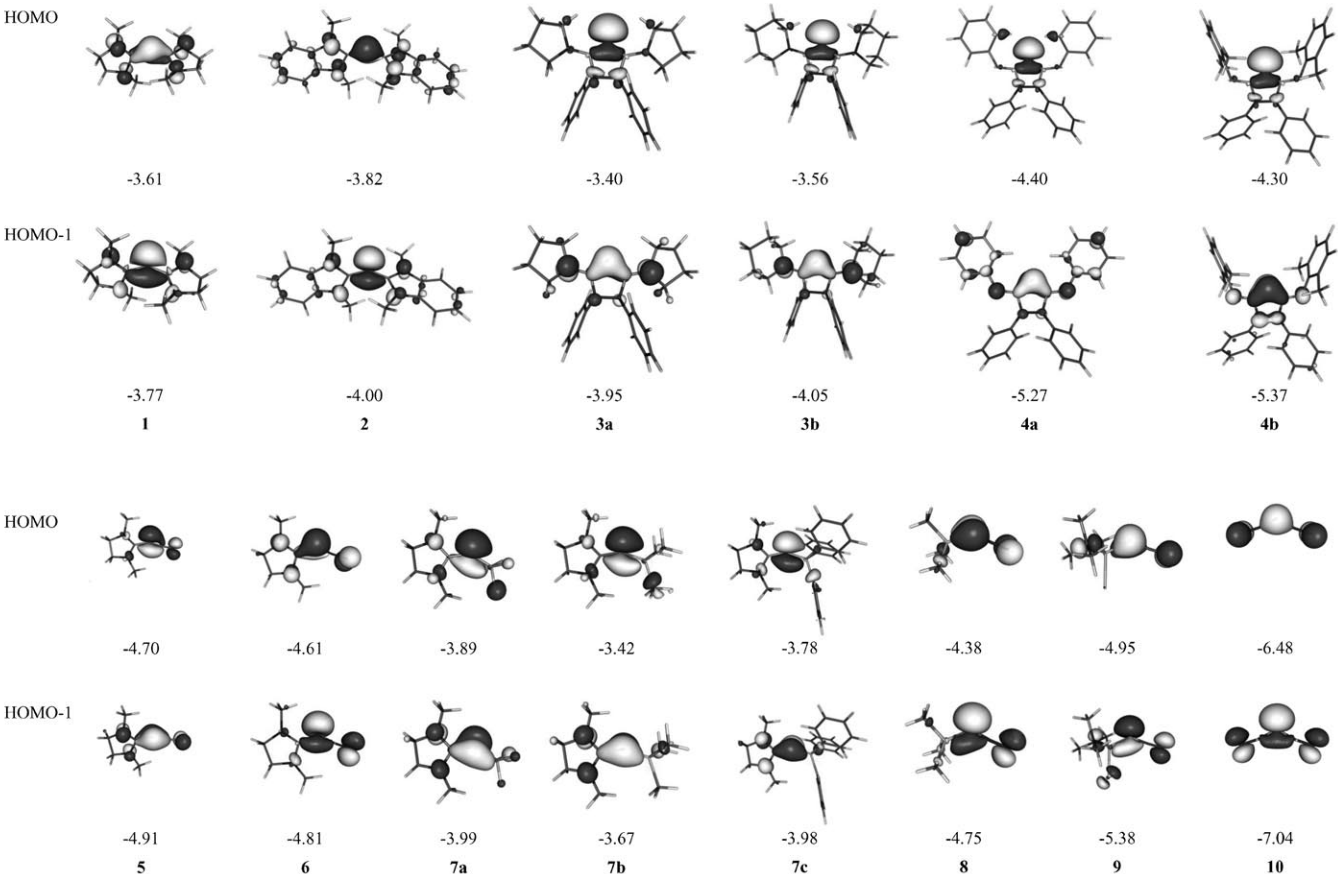

Figure 2. Shape and eigenvalues [eV] of the highest lying occupied molecular orbitals HOMO and HOMO−1 of **1**–**10** at the BP86/SVP level.

Table 2. NBO results at the BP86/TZVPP level//BP86/SVP for CLL′ compounds **1**–**10**. Partial charges and occupation numbers for the central atom q(C1) and for the adjacent atoms E and E′ are given in electrons.

	q(C1)	q(E)/q(E′)[a]	$\mathrm{LP(C1)}_{\sigma}$[b,e]	$\mathrm{LP(C1)}_{\pi}$[c,e]	Residual density[d,e]
1	−0.40	0.30/0.30	−(1.36)[f]	(1.14)	1.7% (2.9%)
2	−0.43	0.31/0.31	−(1.37)[f]	(1.16)	2.8% (3.6%)
3a	−0.48	0.31/0.31	1.78 (1.59)[g]	(0.91)	2.6% (2.8%)
3b	−0.49	0.31/0.31	1.78 (1.60)[g]	(0.91)	2.3% (3.1%)
4a	−0.49	0.43/0.43	1.77 (1.54)[g]	(0.91)	3.2% (3.6%)
4b	−0.48	0.43/0.43	1.77 (1.50)[g]	(0.90)	2.9% (3.3%)
5	−0.52	0.38/0.54	−(1.36)[f]	(1.18)	2.4% (3.0%)
6	−0.25	0.33/−0.01	1.40 (1.43)[h]	(1.10)	2.7% (3.4%)
7a	−0.89	0.33/0.76	1.59 (1.54)[h]	(1.25)	2.0% (2.5%)
7b	−0.95	0.33/1.50	1.57 (1.55)[h]	(1.26)	1.6% (2.1%)
7c	−0.91	0.34/1.49	1.54 (1.50)[h]	(1.27)	2.8% (3.0%)
8	−0.67	1.48/0.00	1.40	1.30	2.6%
9	−0.70	1.76/0.02	1.37	1.31	2.2%
10	−0.05	0.00	1.33	1.13	5.0%

[a] Atoms E/E′ which are directly bonded to the central carbon. [b] Occupation number of the σ lone pair at C1. [c] Occupation number of the π lone pair at C1. [d] Density that is left after the diagonalization step resulting in the NBOs. Given as total non-Lewis contribution in the NBO calculation. [e] Values in parentheses come from Lewis structures with two lone pairs at the central carbon atom, enforced in the NBO calculations. [f] Best Lewis structure given in NBO shows two C1=E/E' bonds. [g] Best Lewis structure given in NBO shows a E-C-E′ 3c2e bond. [h] Best Lewis structure given in NBO shows one C=E and one C−E′ bond.

symmetry and that the energetically lower lying HOMO−1 is a σ-type orbital, while the HOMO and HOMO−1 of the other molecules have a reversed order with respect to σ and π symmetry. Inspection of the ligands at the central carbon atom indicates that those systems in which the ligand is a poor π acceptor like N_2 in **6** and **8**–**10** have a π HOMO, while complex **5** with the better π-acceptor ligand CO and systems **3**, in which the two-coordinate carbon systems is part of a 6π Hückel aromatic system, stabilize the highest lying π MO, which becomes the HOMO−1.

The NBO analysis makes it possible to identify the nature of the two highest lying orbitals as lone-pair orbital or as bonding orbital, and it is also possible to quantify the extent of delocalization. Table 2 shows that the standard NBO calculations identify the σ orbitals as lone-pair orbitals with occupation numbers of greater than 1.3 electrons for all compounds except **1**, **2**, and **6**, which are calculated to exhibit two C=E bonds. The π orbitals are identified as lone-pair orbitals only for **8**–**10** by the standard NBO calculations. For the other molecules, the π orbitals are bonding orbitals of the central carbon atom with ligand atoms, either as a double bond or in a 3c2e bond. It is possible to enforce both orbitals to be localized at the central carbon atom for **1**–**7** as well. Table 2 shows that the residual electron density increases only slightly when this localization is enforced. The occupation of the π-type lone pair orbitals is in all cases smaller than that of the σ lone pair. Thus, the NBO method reveals the extent of the carbone character for compounds **1**–**10**.

The atomic partial charges listed in Table 2 are further support for a description of the bonding situation L→C←L′ for **1**–**10**. The NBO calculations suggest that carbon always carries a negative partial charge, which comes from the donation of the σ lone-pair orbitals of the ligands. This is remarkable, because in the case of **6** and **8**–**10** the bonded donor atom nitrogen is more electronegative than carbon. Even in the homoleptic complex $C(N_2)_2$, the carbon atom carries a small negative charge of −0.05 e, while the N_2 ligands are slightly positively charged. Thus, $N_2 \rightarrow C \leftarrow N_2$ σ donation is stronger than $N_2 \leftarrow C \rightarrow N_2$ π backdonation. Note that the carbene carbon atom in the parent NHC carries a small positive charge of +0.04 e while the attached nitrogen atoms have a large negative charge of −0.53 e.[5] It is also noteworthy that substitution of one NHC ligand of **1** by CO yielding **5** enhances the negative partial charge at the central carbon atom from −0.40 e to −0.52 e, while the substitution by N_2 yielding **6** significantly lowers the partial charge to −0.25 e (Table 2). Replacement of one NHC ligand in **1** by a phosphane group yielding **7a**–**7c** gives much higher negative partial charges at the carbon atom. The calculated values are between −0.89 e and −0.95 e. Note that the stronger charge donation $R_3P \rightarrow C \leftarrow PR_3$ in **7a**–**7c** compared with the donation NHC→C←NHC in **1** does not mean that the bonds in the former compounds are stronger than in the latter. Table 1 shows that the BDE of **1** is significantly higher than those of **7a**–**7c**. The calculated charge distribution shown in Table 2 is in accord with the description of the chemical bonds at the central carbon atom in **1**–**10** in terms of donor–acceptor interactions.

Proton affinities: Previous studies have shown that the second proton affinity (PA) is a sensitive probe for the divalent carbon(0) character of a molecule, because donor compounds which can provide a second lone pair orbital at carbon have large values of both the first and second PA.[7] Table 3 shows the calculated first and second PAs of **1**–**10** at the MP2/TZVPP//BP86/SVP level of theory, which was used in our previous studies.[4,7] The values refer to protonation at the central carbon atom. Test calculations have shown that carbon protonation is always energetically more favorable than protonation at any heteroatom which carries a lone-pair orbital (O, N, Cl). Table 3 gives for comparison also the first and second proton affinities of the carbodiphosphoranes $C(PH_3)_2$, $C(PMe_3)_2$, and $C(PPh_3)_2$, the carbodicarbene bearing unsaturated NHC ligands $\mathrm{C(NHC}^{\mathrm{u}}_{\mathrm{Me}})_2$, and carbon suboxide $C(CO)_2$, which have been studied by us before.[4,7]

The theoretical PA values in Table 3 suggest that compounds **1**–**9** are very basic and should be classified as superbases according to the definition of Raczýnska et al. (PA > 1000 kJ mol^{-1} ≈ 239 kcal mol^{-1}).[49] Bis(diaza)carbone $C(N_2)_2$ (**10**) has a much smaller first PA than the other compounds

Table 3. First and second PAs of **1**–**10** [kcal mol^{-1}] at the MP2/TZVPP//BP86/SVP level of theory. Atomic partial charges at the central carbon atom *q*(C1) in the singly and doubly protonated species (BP86/TZVPP//BP86/SVP).

Molecule	**M**–(H$^+$)		**M**-(H$^+$)$_2$	
	1st PA	*q*(C1)	2nd PA	*q*(C1)
1	282.2	−0.48	157.5	−0.54
2	284.7	−0.51	167.8	−0.53
3a	296.5	−0.42	158.7	−0.52
3b	293.5	−0.42	158.0	−0.53
4a	285.2	−0.43	131.0	−0.61
4b	284.3	−0.44	133.3	−0.61
5	243.3	−0.58	99.0	−0.65
6	244.1	−0.29	111.5	−0.35
7a	273.3	−0.85	140.2	−0.75
7b	284.2	−0.88	160.4	−0.78
7c	287.1	−0.86	176.4	−0.78
8	243.5	−0.63	108.4	−0.60
9	239.7	−0.68	115.5	−0.63
10	195.6	−0.11	47.0	−0.18
$C(PH_3)_2$[a]	255.7	−1.26	114.4	−1.01
$C(PMe_3)$[a]	278.4	−1.36	156.2	−1.07
$C(PPh_3)_2$[a]	280.0	−1.33	185.6	−1.07
$C(CO)_2$[a]	182.5	−0.67	28.7	−0.74
$C(NHC^{u}_{Me})_2$[a]	294.3	−0.52	168.4	−0.53

[a] Proton affinities were taken from reference [4], and partial charges from reference [6].

of only 195.6 kcal mol^{-1}. The largest values for the first PA are predicted for cyclic species **3a** and **3b**. The most interesting data for our study are the calculated values for the second PA. Table 3 shows that the theoretically predicted second PAs of **1**–**9** are rather high, particularly for compounds **1**–**3**, **7b**, and **7c**. Note that the order of the second PA of the carbon bases is not the same as for the first PA. This observation has been made before.[7] The first PA refers to neutral species **1**–**10** and is mainly determined by the energy level of the highest lying occupied σ orbital, while the second PA is mainly determined by the highest lying occupied π orbital of the protonated species **1**(H$^+$)–**10**(H$^+$), which is always the HOMO.

The highest second PA is calculated for the mixed complex $C(NHC^{s}_{Me})(PPh_3)$ (**7c**) and not for **3a** and **3b**, which have the largest values of the first PA. The calculations suggest that the first and second PA of the carbodicarbene bearing saturated NHC ligands $C(NHC^{s}_{Me})_2$ (**1**) are slightly smaller than those of $C(NHC^{u}_{Me})_2$. Interestingly, the first PA of mixed carbone $C(NHC^{s}_{Me})(PPh_3)$ (**7c**) is larger than those of homoleptic carbones **1** and $C(PPh_3)_2$, but the second PA of $C(PPh_3)_2$ is larger. The same observation can be made for the proton affinities of the mixed carbone **7b** in comparison with **1** and $C(PMe_3)_2$. On the other hand, mixed carbone $C(NHC^{s}_{Me})(PH_3)$ (**7a**) has lower proton affinities than **1**, which can be explained by the rather low PA values of $C(PH_3)_2$. Compounds **3a** and **3b** may be considered as carbones in which the divalent C^0 atom is bonded to two diaminocarbene ligands $C(NR_2)_2$, while **4a** and **4b** have two oxoaminocarbene ligands $C(NR_2)(OR)$. The latter ligands are weaker donors than the former, and this explains why the first and second PAs of **3a** and **3b** are higher than those of **4a** and **4b**.

The first and the second PAs of $C(N_2)_2$ (**10**) are slightly larger than those of $C(CO)_2$. This is interesting because **10** has a strongly bent geometry with a bending angle of 124.6°, while carbon suboxide is quasilinear.[50] However, the bending potentials of both compounds are very shallow, as is typical of molecules CL_2 which have divalent carbon(0) character.[3–5,16] The calculated proton affinities show that $C(N_2)_2$ (**10**) and $C(CO)_2$ do not exhibit the characteristic chemical reactivity of a carbone which has very large first and second PAs. Furthermore, the second PAs of **5**, **6**, **8**, and **9** are clearly smaller than those of the other molecules (Table 3), and the assignment of these compounds as carbones may be questioned. However, it will be shown below that these species all yield stable 1:2 complexes with Lewis acidic BH_3. This distinguishes them from NHCs, which bind only one BH_3 molecule. According to the theoretical results, all compounds **1**–**10** have carbon(0) character, which is particularly strong in **1**–**3**, **7b**, and **7c**. All complexes which bear CO or N_2 as a ligand have comparatively small values of the second PA.

Table 3 also lists the atomic partial charges of the central carbon atom in the protonated and diprotonated species. It is noteworthy that the carbon atoms remain negatively charged even after double protonation. This observation has been made before.[3–5,16] It can be explained by the increased charge at the carbon atom after protonation, which changes the polarization of the $L \rightarrow C(H^+)_n$ bonds towards the carbon atom. The charge shift compensates for the loss of electronic charge of carbon to the proton. The partial charge at carbon in the protonated species may even be more negative than in the neutral molecule. This holds for example for compounds **1**, **2**, **5**, **6**, and **10**, in which the absolute value of the negative partial charge at the central carbon atoms increases from the neutral compound to the singly protonated species and further to the doubly protonated complex.

Figure 3a shows a correlation between the eigenvalues of the HOMO of **1**–**10** and the first PAs, and Figure 3b the correlation between ε(HOMO) of the singly protonated species **1**(H$^+$)–**10**(H$^+$) and the second PAs. The correlation coefficients of about 0.88 and about 0.93, respectively, suggest that the first and second PAs are mainly determined by the energy level of the highest lying σ orbital of compounds **1**–**10** and the π HOMO of the singly protonated species, respectively, but other factors such as the electrostatic interaction also play a role. For example, the HOMO of **1** is much higher in energy (−3.61 eV) than the HOMO of **4a** (−4.40 eV), and yet the latter has a slightly larger first PA (285.2 kcal mol^{-1}) than the former (282.2 kcal mol^{-1}). The same finding was reported in a recent analysis of the first and second proton affinities of carbon bases.[7]

Complexes of 1–10 with BH_3: Another characteristic feature of divalent carbon(0) compounds which distinguishes them from carbenes is the ability of the central carbon atom to

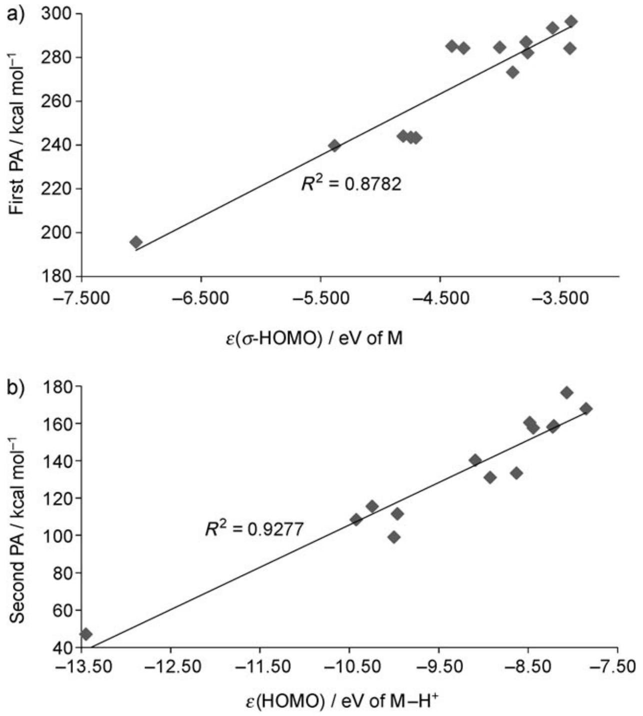

Figure 3. a) Correlation between the first proton affinity of **M** and the eigenvalue of the highest lying occupied σ orbital. b) Correlation between the second proton affinity of **M** and the eigenvalue of the highest lying occupied π orbital (HOMO) of **M**-(H^+).

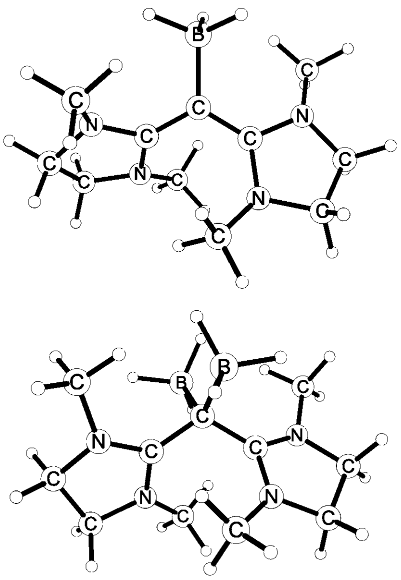

Figure 4. Optimized structures of **1**-BH_3 (top) and **1**-$(BH_3)_2$ (bottom).

Table 4. Dissociation energies D_e of complexes **M**-BH_3 and **M**-$(BH_3)_2$ at the MP2/TZVPP//BP86/SVP level. Free energies ΔG are given in parentheses. Calculated C−BH_3 bond lengths [Å] at the BP86/SVP level. All energies are given in kcal mol^{-1}.

	M-BH_3→M+BH_3			BH_3-M-BH_3→M-BH_3+BH_3		
	D_e	(−ΔG)	r(C−BH_3)	D_e	(−ΔG)	r(C−BH_3)
1	42.1	(26.1)	1.673	29.0	(13.0)	1.741
2	49.3	(32.1)	1.667	27.0	(11.3)	1.743
3a	58.4	(42.7)	1.633	20.0	(5.8)	1.732/1.779
3b	57.6	(42.2)	1.629	16.9	(1.7)	1.762/1.763
4a	53.9	(40.0)	1.616	5.7	(−8.9)	1.674/2.032
4b	53.0	(38.2)	1.621	9.5	(−4.5)	1.647/2.094
5	30.7	(15.7)	1.701	17.4	(3.6)	1.757/1.819
6	31.9	(18.0)	1.673	20.7	(6.3)	1.763/1.788
7a	46.9	(31.9)	1.653	33.8	(18.1)	1.718/1.741
7b	51.7	(36.0)	1.655	26.4	(10.2)	1.733/1.750
7c	48.0	(31.4)	1.662	23.6	(7.3)	1.733/1.767
8	35.9	(22.2)	1.669	30.2	(15.4)	1.742
9	34.8	(21.8)	1.669	22.6	(7.5)	1.737/1.763
10	22.2	(10.0)	1.673	14.7	(1.6)	1.777

bind two main-group Lewis acids.[3,4,6] For example, theoretical calculations suggested that carbodiphosphorane $C(PPh_3)_2$ should bind two BH_3 ligands in the complex $C(PPh_3)_2(BH_3)_2$, in which the second borane ligand still has a BDE of $D_0^{298}=15.8$ kcal mol^{-1}.[3] The theoretical prediction was recently confirmed by the isolation of the complex $[\{C(PPh_3)_2\}\{(\mu\text{-}H)H_4B_2\}]^+$,[51] which was synthesized by reaction of $C(PPh_3)_2$ with B_2H_6, whereby one hydride ligand dissociates from the proposed intermediate $C(PPh_3)_2(BH_3)_2$ and reacts with excess B_2H_6 yielding $B_2H_7^-$ as counterion.

We calculated the complexes of the Lewis **1**–**10** with one and two BH_3 molecules as Lewis acids. The optimized structures of **1**-BH_3 and **1**-$(BH_3)_2$ are shown in Figure 4. The borane adducts of the other compounds **2**–**10** show similar features and thus are not shown here. The structures of **M**-BH_3 and **M**-$(BH_3)_2$ (**M** = **2**–**10**) are shown in Figure S2 of the Supporting Information. The first BH_3 ligand always binds to the σ lone pair of carbon, while the complexes with two borane molecules exhibit a tetrahedral arrangement at the carbon atom. This is similar to the previously investigated complexes $L_2C(BH_3)_2$.[6] We note that the heavier Group 14 homologues L_2E (E = Si–Sn) are predicted to bind the first Lewis acid through the π-type lone pair at atom E. Calculations show that main group Lewis acids, proton, and transition metal fragments are bonded to atom E of L_2E out of the L-E-L plane.[52]

Table 4 lists the calculated bond energies D_e and free energies $-\Delta G$ (negative by sign convention) at the MP2/TZVPP//BP86/SVP level for loss of one and two BH_3 ligands from **M**-BH_3 and **M**-$(BH_3)_2$ (**M** = **1**–**10**). The theoretically predicted C−BH_3 distances of the equilibrium structures are also given. The calculations predict that all singly coordinated complexes **M**-BH_3 should be stable enough to be isolated in a condensed phase. The BDEs of complexes **1**–**4** and **7** are greater than 40 kcal mol^{-1}, which places them among the most strongly bonded donor–acceptor complexes of main group elements.[53] The most strongly bonded BH_3 complexes **M**-BH_3 correlate with the compounds **M** which have the highest PA (Table 3), although the order is not always the same (e.g., **7b** and **7c**). Note that the C−BH_3 bond length does not correlate with the bond dissociation energy. Compounds **1** and **10** have the same bond length of $r(B{-}CH_3) = 1.673$ Å, but the BDE of **1** ($D_e = 42.1$ kcal mol^{-1}) is nearly twice as large as the BDE of **10** ($D_e = 22.2$ kcal mol^{-1}). The equilibrium distance of a covalent bond depends on the interplay of orbital interactions, electrostatic bonding, and Pauli repulsion,[48a,b] which may even lead to a situation in which a chemical bond between two atoms in one molecule may be shorter and yet weaker than in the other.[54]

Table 4 shows that most compounds **1**–**10** bind a second BH_3 ligand strongly enough that the complex might be isolated in a condensed phase. The BDE for the second BH_3 ligand of **4a**-$(BH_3)_2$ and **4b**-$(BH_3)_2$ is very small, and the free energies are even negative, probably due to steric repulsion between the borane ligands and the bulky substituents. Substituted homologues $C(PR_3)(N_2)$ of **8** and **9** are experimentally known, and it would be interesting to let them react with diborane. The calculations predict that **8** and **9** should strongly bind one but also two BH_3 ligands. Inspection of the first and second PAs and the BDEs for one and two BH_3 ligands show (Tables 3 and 4) that the trend for binding one molecule of BH_3 is similar to that of the first PA, but there is no correlation between the second PA and the BDE of the second BH_3 ligand. This is most likely due to steric hindrance for adding a second borane ligand to the complexes.

We analyzed the nature of the **M**-BH_3 bonds with the EDA method (Table 5). Note that the EDA calculations have been carried out at a different level of theory (BP86/TZ2P with Slater-type basis functions) to the above calculations (MP2/TZVPP//BP86/SVP with Gaussian-type basis functions), and thus the calculated BDEs are slightly different. However, the trends of the BDEs are very similar. The optimized geometries at the BP86/TZ2P level with Slater-type basis functions are also rather similar to the BP86/SVP optimized structures. The full sets of coordinates are given in the Supporting Information.

The EDA results show that the intrinsic interaction energy between the frozen fragments ΔE_{int} is significantly higher than the BDE owing to structural relaxation of the fragments. This holds in particular for the BH_3 fragment, the planar equilibrium geometry of which is distorted toward pyramidal in the complexes **M**-BH_3. Table 5 shows that the ΔE_{prep} values for BH_3 are rather high. The breakdown of the interaction energy ΔE_{int} into its bonding contributions shows that the percentage contribution of the electrostatic term ΔE_{elstat} varies between 48.7 % in **3a** and 38.3 % in **10**. The C–BH_3 bond in the latter compound has a smaller electrostatic character than in **1**. This explains the above observation that **1** and **10** have the same C–BH_3 bond length but the bond strength in **1** is much higher than in **10**. Table 5 shows that the percentage contribution ΔE_{elstat} correlates quite well with the total interaction energy ΔE_{int}. Compound **3a** has the largest electrostatic character (48.7 % ΔE_{elstat}) and it has the largest ΔE_{int} value (−83.1 kcal mol^{-1}), while the smallest electrostatic character in **10** (38.3 % ΔE_{elstat}) correlates with the smallest ΔE_{int} value (−37.1 kcal mol^{-1}).

Table 5. EDA results (BP86/TZ2P) of complexes **M**-BH_3. The interacting fragments are **M** and BH_3.

	1	**2**	**3a**	**4a**	**5**	**6**
ΔE_{int}	−70.4	−69.8	−83.1	−73.7	−49.5	−56.1
ΔE_{Pauli}	142.4	143.9	161.9	150.3	123.7	126.0
ΔE_{elstat}[a]	−94.8 (44.5 %)	−95.8 (44.8 %)	−119.3 (48.7 %)	−104.8 (46.8 %)	−74.4 (43.0 %)	−78.8 (43.3 %)
ΔE_{orb}[a]	−118.0 (55.5 %)	−117.9 (55.2 %)	−125.7 (51.3 %)	−119.2 (53.2 %)	−98.8 (57.0 %)	−103.3 (56.7 %)
ΔE_{prep}	33.3	30.7	27.8	26.7	21.8	22.8
ΔE_{prep}(M)	10.4	8.2	4.9	6.7	4.8	5.8
$\Delta E_{prep}(BH_3)$	22.9	22.5	22.9	20.0	17.0	17.0
$\Delta E=-D_e$	−37.1	−39.1	−55.3	−47.0	−27.7	−33.3

	7a	**7b**	**7c**	**8**	**9**	**10**
ΔE_{int}	−74.7	−77.8	−70.7	−57.0	−53.3	−37.1
ΔE_{Pauli}	163.0	155.4	153.2	125.6	124.0	107.1
ΔE_{elstat}[a]	−111.2 (46.8 %)	−109.9 (47.1 %)	−102.0 (45.6 %)	−78.3 (42.9 %)	−74.7 (42.1 %)	−55.3 (38.3 %)
ΔE_{orb}[a]	−126.5 (53.2 %)	−123.3 (52.9 %)	−121.8 (54.4 %)	−104.3 (57.1 %)	−102.6 (57.9 %)	−89.0 (61.7 %)
ΔE_{prep}	30.4	32.1	31.9	20.1	20.6	13.0
ΔE_{prep}(M)	7.4	9.0	9.1	2.7	3.6	1.3
$\Delta E_{prep}(BH_3)$	22.9	23.2	22.7	17.4	16.9	11.7
$\Delta E=-D_e$	−44.3	−45.7	−38.8	−36.9	−32.7	−24.1

[a] The values in parentheses are the percentage contributions to the total attractive interactions $\Delta E_{elstat}+\Delta E_{orb}$.

Conclusion

Charge- and energy-decomposition analysis of the electronic structure of compounds **1**–**10** reveals divalent carbon(0) character in different degrees for all molecules. A carbone-type bonding situation L→C←L is particularly strong for carbodicarbenes **1** and **2**, "bent allenes" **3a**, **3b**, **4a**, **4b**, and carbocarbenephosphoranes **7a**, **7b**, and **7c**. The last-named compounds have both very large first and second proton affinities. They also bind two BH_3 ligands with bond energies which are high enough that the bis-adducts should be isolable in a condensed phase. The second proton affinities of complexes **5**, **6**, **8**–**10** bearing CO or N_2 as ligand are significantly lower than those of the other compounds. However, they give stable complexes with two BH_3 ligands, and this shows that they are twofold Lewis bases. The chemistry of carbones is different from that of carbenes because divalent carbon(0) compounds CL_2 are π donors, and thus they may serve as double Lewis bases, while divalent carbon(II) compounds are π acceptors. The theoretical results point toward new directions for experimental research in the field of low-coordinate carbon compounds.

Acknowledgements

We are grateful to the referees for helpful comments which improved the manuscript. This work was supported by the Deutsche Forschungsgemeinschaft. Excellent service by the Hochschulrechenzentrum of the Philipps-Universität Marburg is gratefully acknowledged. Further computer time was provided by the HLR Stuttgart, the CSC Frankfurt and the HHLR Darmstadt.

---

[1] W. Petz, C. Kutschera, M. Heitbaum, G. Frenking, R. Tonner, B. Neumüller, *Inorg. Chem.* **2005**, *44*, 1263.

[2] S. Marrot, T. Kato, F. P. Cossio, H. Gornitzka, A. Baceiredo, *Angew. Chem.* **2006**, *118*, 7607; *Angew. Chem. Int. Ed.* **2006**, *45*, 7447.

[3] R. Tonner, F. Öxler, B. Neumüller, W. Petz, G. Frenking, *Angew. Chem.* **2006**, *118*, 8206; *Angew. Chem. Int. Ed.* **2006**, *45*, 8038.

[4] R. Tonner, G. Frenking, *Angew. Chem.* **2007**, *119*, 8850; *Angew. Chem. Int. Ed.* **2007**, *46*, 8695.

[5] R. Tonner, G. Frenking, *Chem. Eur. J.* **2008**, *14*, 3260.

[6] R. Tonner, G. Frenking, *Chem. Eur. J.* **2008**, *14*, 3273.

[7] R. Tonner, G. Heydenrych, G. Frenking, *ChemPhysChem* **2008**, *9*, 1474.

[8] M. Jablonski, M. Palusiak, *PhysChemComm* **2009**, *11*, 5711.

[9] M. Hänninen, A. Peuronen, H. M. Tuononen, *Chem. Eur. J.* **2009**, *15*, 7287.

[10] M. Alcarazo, C. W. Lehmann, A. Anoop, W. Thiel, A. Fürstner, *Nat. Chem. Biol.* **2009**, *1*, 295.

[11] I. Fernandez, C. A. Dyker, A. DeHope, B. Donnadieu, G. Frenking, G. Bertrand, *J. Am. Chem. Soc.* **2009**, *131*, 11 875.

[12] C. A. Dyker, V. Lavallo, B. Donnadieu, G. Bertrand, *Angew. Chem.* **2008**, *120*, 3250; *Angew. Chem. Int. Ed.* **2008**, *47*, 3206.

[13] A. Fürstner, M. Alcarazo, R. Goddard, C. W. Lehmann, *Angew. Chem.* **2008**, *120*, 3254; *Angew. Chem. Int. Ed.* **2008**, *47*, 3210.

[14] V. Lavallo, C. A. Dyker, B. Donnadieu, G. Bertrand, *Angew. Chem.* **2008**, *120*, 5491; *Angew. Chem. Int. Ed.* **2008**, *47*, 5411.

[15] O. Kaufhold, E. E. Hahn, *Angew. Chem.* **2008**, *120*, 4122; *Angew. Chem. Int. Ed.* **2008**, *47*, 4057.

[16] R. Tonner, G. Frenking, *Pure Appl. Chem.* **2009**, *81*, 597.

[17] H. G. Viehe, Z. Janousek, R. Gompper, D. Lach, *Angew. Chem.* **1973**, *85*, 581; *Angew. Chem. Int. Ed. Engl.* **1973**, *12*, 566.

[18] M. Christl, B. Engels, *Angew. Chem.* **2009**, *121*, 1566; *Angew. Chem. Int. Ed.* **2009**, *48*, 1538.

[19] V. Lavallo, C. A. Dyker, B. Donnadieu, G. Bertrand, *Angew. Chem.* **2009**, *121*, 1568; *Angew. Chem. Int. Ed.* **2009**, *48*, 1540.

[20] a) J.-M. Sotiropoulos, A. Baceiredo, G. Bertrand, *J. Am. Chem. Soc.* **1987**, *109*, 4711; b) N. DubauAssibat, A. Baceiredo, F. Dahan, G. Bertrand, *Bull. Soc. Chim. Fr.* **1995**, *132*, 1139; c) J. M. Sotiropoulos, A. Baceiredo, G. Bertrand, *Bull. Soc. Chim. Fr.* **1992**, *129*, 367.

[21] H. J. Bestmann, *Angew. Chem.* **1977**, *89*, 361; *Angew. Chem. Int. Ed. Engl.* **1977**, *16*, 349.

[22] A. Igau, H. Grützmacher, A. Baceiredo, G. Bertrand, *J. Am. Chem. Soc.* **1988**, *110*, 6463.

[23] a) A. Igau, A. Baceiredo, G. Trinquier, G. Bertrand, *Angew. Chem.* **1989**, *101*, 617; *Angew. Chem. Int. Ed. Engl.* **1989**, *28*, 621; b) T. Kato, H. Gornitzka, A. Baceiredo, A. Savin, G. Bertrand, *J. Am. Chem. Soc.* **2000**, *122*, 998; c) D. Bourissou, O. Guerret, F. P. Gabbai, G. Bertrand, *Chem. Rev.* **2000**, *100*, 39.

[24] P. Pyykkö, N. Runeberg, *J. Mol. Struct.* **1991**, *242-264*, 279.

[25] Gaussian 03, Revision D.01, M. J. Frisch, G. W. Trucks, H. B. Schlegel, G. E. Scuseria, M. A. Robb, R. J. Cheeseman, J. A. Montgomery, Jr., T. Vreven, K. N. Kudin, J. C. Burant, J. M. Millam, S. S. Iyengar, J. Tomasi, V. Barone, B. Mennucci, M. Cossi, G. Scalmani, N. Rega, G. A. Petersson, H. Nakatsuji, M. Hada, M. Ehara, K. Toyota, R. Fukuda, J. Hasegawa, M. Ishida, T. Nakajima, Y. Honda, O. Kitao, H. Nakai, M. Klene, X. Li, J. E. Knox, H. P. Hratchian, J. B. Cross, V. Bakken, C. Adamo, J. Jaramillo, R. Gomperts, R. E. Stratmann, O. Yazyev, A. J. Austin, R. Cammi, C. Pomelli, J. W. Ochterski, P. Y. Ayala, K. Morokuma, G. A. Voth, P. Salvador, J. J. Dannenberg, V. G. Zakrzewski, S. Dapprich, A. D. Daniels, M. C. Strain, O. Farkas, D. K. Malick, A. D. Rabuck, K. Raghavachari, J. B. Foresman, J. V. Ortiz, Q. Cui, A. G. Baboul, S. Clifford, J. Cioslowski, B. B. Stefanov, G. Liu, A. Liashenko, P. Piskorz, I. Komaromi, R. L. Martin, D. J. Fox, T. Keith, M. A. Al-Laham, C. Y. Peng, A. Nanayakkara, M. Challacombe, P. M. W. Gill, B. Johnson, W. Chen, M. W. Wong, C. Gonzalez, J. A. Pople, Gaussian Inc.: Wallingford, CT, **2004**.

[26] C. Peng, P. Y. Ayala, H. B. Schlegel, M. J. Frisch, *J. Comput. Chem.* **1996**, *17*, 49.

[27] R. Ahlrichs, M. Bär, M. Häser, H. Horn, C. Kälmel, *Chem. Phys. Lett.* **1989**, *162*, 165.

[28] a) A. D. Becke, *Phys. Rev. A* **1988**, *38*, 3098; b) J. P. Perdew, *Phys. Rev. B* **1986**, *33*, 8822.

[29] A. Schäfer, H. Horn, R. Ahlrichs, *J. Chem. Phys.* **1992**, *97*, 2571.

[30] a) C. Møller, M. S. Plesset, *Phys. Rev. A* **1934**, *46*, 618; b) J. S. Binkley, J. A. Pople, *Int. J. Quantum Chem.* **1975**, *9S*, 229.

[31] F. Weigend, R. Ahlrichs, *Phys. Chem. Chem. Phys.* **2005**, *7*, 3297.

[32] a) J. J. Cizek, *Chem. Phys.* **1966**, *45*, 4256; b) J. A. Pople, K. Raghavachari, H. B. Schlegel, J. S. Binkley, *Int. J. Quantum Chem.* **1978**, *14*, 545; c) R. J. Bartlett, G. D. Purvis, *Int. J. Quantum Chem.* **1978**, *14*, 561; d) G. D. Purvis, R. J. Bartlett, *J. Chem. Phys.* **1982**, *76*, 1910; e) K. Raghavachari, G. W. Trucks, J. A. Pople, M. Head-Gordon, *Chem. Phys. Lett.* **1989**, *157*, 479; f) R. J. Bartlett, J. D. Watts, S. A. Kucharski, J. Noga, *Chem. Phys. Lett.* **1990**, *165*, 513; g) C. Hampel, K. Peterson, H.-J. Werner, *Chem. Phys. Lett.* **1992**, *190*, 1; h) J. D. Watts, J. Gauss, R. J. Bartlett, *J. Chem. Phys.* **1993**, *98*, 8718; i) MOLPRO, version 2006.1, a package of ab initio programs, H.-J. Werner, P. J. Knowles, R. Lindh, F. R. Manby, M. Schütz, see http://www.molpro.net.

[33] a) K. Eichkorn, O. Treutler, H. Ohm, M. Häser, R. Ahlrichs, *Chem. Phys. Lett.* **1995**, *242*, 652; b) F. Weigend, *Phys. Chem. Chem. Phys.* **2006**, *8*, 1057; c) F. Weigend, M. Häser, *Theor. Chem. Acc.* **1997**, *97*, 331; d) F. Weigend, M. Häser, H. Patzelt, R. Ahlrichs, *Chem. Phys. Lett.* **1998**, *294*, 143.

[34] a) S. Grimme, *J. Chem. Phys.* **2003**, *118*, 9095; b) S. Grimme, *J. Phys. Chem. A* **2005**, *109*, 3067.

[35] A. E. Reed, F. Weinhold, *J. Chem. Phys.* **1983**, *78*, 4066.

[36] A. E. Reed, R. B. Weinstock, F. Weinhold, *J. Chem. Phys.* **1985**, *83*, 735.

[37] A. E. Reed, L. A. Curtiss, F. Weinhold, *Chem. Rev.* **1988**, *88*, 899.

[38] G. Te Velde, F. M. Bickelhaupt, E. J. Baerends, C. F. Guerra, S. J. A. Van Gisbergen, J. G. Snijders, T. Ziegler, *J. Comput. Chem.* **2001**, *22*, 931.

[39] E. Van Lenthe, E. J. Baerends, *J. Comput. Chem.* **2003**, *24*, 1142.

[40] J. Krijn, E. J. Baerends, Fit Functions in the HFS-Method, Internal Report (in Dutch); Vrije Universiteit Amsterdam, Amsterdam, **1984**.

[41] E. Van Lenthe, E. J. Baerends, J. G. Snijders, *J. Chem. Phys.* **1994**, *101*, 9783.

[42] E. van Lenthe, A. Ehlers, E. J. Baerends, *J. Chem. Phys.* **1999**, *110*, 8943.

[43] K. Morokuma, *J. Chem. Phys.* **1971**, *55*, 1236.

[44] T. Ziegler, A. Rauk, *Theor. Chem. Acc.* **1977**, *46*, 333.

[45] F. M. Bickelhaupt, E. J. Baerends, *Rev. Comput. Chem.* **2000**, *15*, 1.

[46] F. M. Bickelhaupt, N. M. M. Nibbering, E. M. V. Wezenbeek, E. J. Baerends, *J. Phys. Chem.* **1992**, *96*, 4864.

[47] a) G. Frenking, K. Wichmann, N. Fröhlich, C. Loschen, M. Lein, J. Frunzke, V. M. Rayón, *Coord. Chem. Rev.* **2003**, *55*, 238; b) M. Lein, G. Frenking, *Theory and Applications of Computational Chemistry: The First 40 Years*. Elsevier, Amsterdam, **2005**, p. 367.

[48] a) C. Esterhuysen, G. Frenking, *Theor. Chem. Acc.* **2004**, *111*, 381; b) A. Kovács, C. Esterhuysen, G. Frenking, *Chem. Eur. J.* **2005**, *11*, 1813; c) A. Krapp, F. M. Bickelhaupt, G. Frenking, *Chem. Eur. J.*

2006, *12*, 9196; d) I. Fernández, G. Frenking, *Chem. Eur. J.* **2006**, *12*, 3617.

[49] E. D. Raczýnska, M. Decouzon, J.-F. Gal, P.-C. Maria, K. Wozniak, R. Kurg, S. N. Carins, *Trends Org. Chem.* **1998**, *7*, 95.

[50] a) P. Jensen, J. W. C. Johns, *J. Mol. Spectrosc.* **1986**, *118*, 248; b) J. Vander Auwera, J. W. C. Johns, O. L. Polyanski, *J. Chem. Phys.* **1991**, *95*, 2299; c) J. Koput, *Chem. Phys. Lett.* **2000**, *320*, 237.

[51] W. Petz, F. Öxler, B. Neumüller, R. Tonner, G. Frenking, *Eur. J. Inorg. Chem.* **2009**, 4507.

[52] a) N. Takagi, T. Shimizu, G. Frenking, *Chem. Eur. J.* **2009**, *15*, 3448; b) N. Takagi, T. Shimizu, G. Frenking, *Chem. Eur. J.* **2009**, *15*, 8593.

[53] a) A. Haaland, *Angew. Chem.* **1989**, *101*, 1017; *Angew. Chem. Int. Ed. Engl.* **1989**, *28*, 992; b) V. Jonas, G. Frenking, M. T. Reetz, *J. Am. Chem. Soc.* **1994**, *116*, 8741.

[54] This has been found for the metal–phosphane bonds in the complexes $(CO)_5M{-}PCl_3$, which are shorter but weaker than in $(CO)_5M{-}PMe_3$ (M = Cr, Mo, W): G. Frenking, K. Wichmann, N. Fröhlich, J. Grobe, W. Golla, D. Le Van, B. Krebs, M. Läge, *Organometallics* **2002**, *21*, 2921.

Received: January 21, 2010